



# Shedding light on biocatalysis: photoelectrochemical platforms for solar-driven biotransformation

Jinhyun Kim and Chan Beum Park

Redox biocatalysis has come to the forefront because of its excellent catalytic efficiency, stereoselectivity, and environmental benignity. The green and sustainable biotransformation can be driven by photoelectrochemical (PEC) platforms where redox biocatalysis is coupled with photoelectrocatalysis. The main challenge is how to transfer photoexcited electrons to (or from) the enzyme redox centers for effective biotransformation using solar energy. This review commences with a conceptual discussion of biocatalytic PEC platforms and highlights recent advances in PEC-based biotransformation through cofactor regeneration or direct transfer of charge carriers to (or from) oxidoreductases on enzyme-conjugated electrodes. Finally, we address future perspectives and potential next steps in the vibrant field of biocatalytic photosynthesis.

## Address

Department of Materials Science and Engineering, Korea Advanced Institute of Science and Technology (KAIST), 335 Science Road, Daejeon 305-701, Republic of Korea

Corresponding author: Park, Chan Beum ([parkcb@kaist.ac.kr](mailto:parkcb@kaist.ac.kr))

**Current Opinion in Chemical Biology** 2019, **49**:122–129

This review comes from a themed issue on **Biocatalysis and biotransformation**

Edited by **Kylie A Vincent** and **Bettina M Nestl**

For a complete overview see the [Issue](#) and the [Editorial](#)

Available online 3rd January 2019

<https://doi.org/10.1016/j.cbpa.2018.12.002>

1367-5931/© 2018 Elsevier Ltd. All rights reserved.

## Introduction

Oxidoreductases (or redox enzymes) can catalyze a wide range of industrially useful redox reactions, such as chiral amine synthesis, asymmetric C=C hydrogenation, C=O reduction, C=C epoxidation, Baeyer–Villiger oxidation of ketones, and CO<sub>2</sub> reduction [1–3]. Redox biocatalysis occurs through the transfer of electrons to (or from) the enzyme prosthetic groups (e.g. flavin, heme, Fe–S cluster) or the adjacent redox centers embedded in the polypeptides. Among the prominent furnishers of electrons are cofactors, such as nicotinamide adenine dinucleotide (NADH) and flavin mononucleotide (FMNH<sub>2</sub>), on which over 80% of oxidoreductases are dependent for their catalytic activities. The stoichiometric provision of

the expensive cofactors, however, makes redox biotransformation processes cost prohibitive; thus, this issue has elicited extensive research on *in situ* regeneration of cofactors using different methods (e.g. enzymatic, chemical, electrochemical, and photochemical) for sustainable reactions catalyzed by oxidoreductases [2,4]. Industrial-scale regeneration of cofactors has been established using secondary enzymes (e.g. glucose dehydrogenase, formate dehydrogenase) and their cosubstrates (e.g. glucose, formate) [5,6]. The enzymatic approach offers high specific activity and biocompatibility, but suffers from the disadvantage of poor atom-efficiency because of stoichiometric requirement of reductants.

Recently, light-driven regeneration of cofactors has received attention as a promising expedient for green biocatalysis because of its merits, such as the use of clean and abundant solar energy, no requirement of secondary enzymes and cosubstrates, and the delivery of photoexcited electrons to hydride-transfer mediators in an atom-efficient manner [4]. In contrast, a direct transfer of photoexcited charge carriers to the prosthetic groups of oxidoreductases has been demonstrated to drive redox biotransformation without relying on the supply of the cofactors [7,8]. These photoexcited charge carriers could be generated by employing semiconducting electrodes (e.g. Pt-modified GaAs, black silicon) [9,10], molecular photosensitizers (e.g. porphyrin-based dyes, xanthene derivatives) [11–13], or particulate semiconductors (e.g. quantum dots, carbon nanodots, carbon nitrides) [14–19] that function as light harvesters and energy transducers.

The use of heterogeneous semiconducting electrodes for the activation of redox enzymes in biocatalytic photoelectrochemical (PEC) platforms has several advantages over homogeneous photocatalytic approaches. For example, an applied bias can tune the Fermi level of the electrons and facilitate a specific endergonic redox reaction in a selective way. Furthermore, the electrical connection between two different semiconducting electrodes through a conducting wire can increase the extent of the absorption spectrum and decrease the electron-hole recombination, thus effectively enhancing the overall productivities of enzymatic reactions coupled with water oxidation.

This review highlights recent advances in the design of biocatalytic PEC platforms for redox biotransformations through the transport of photoexcited electrons to (or

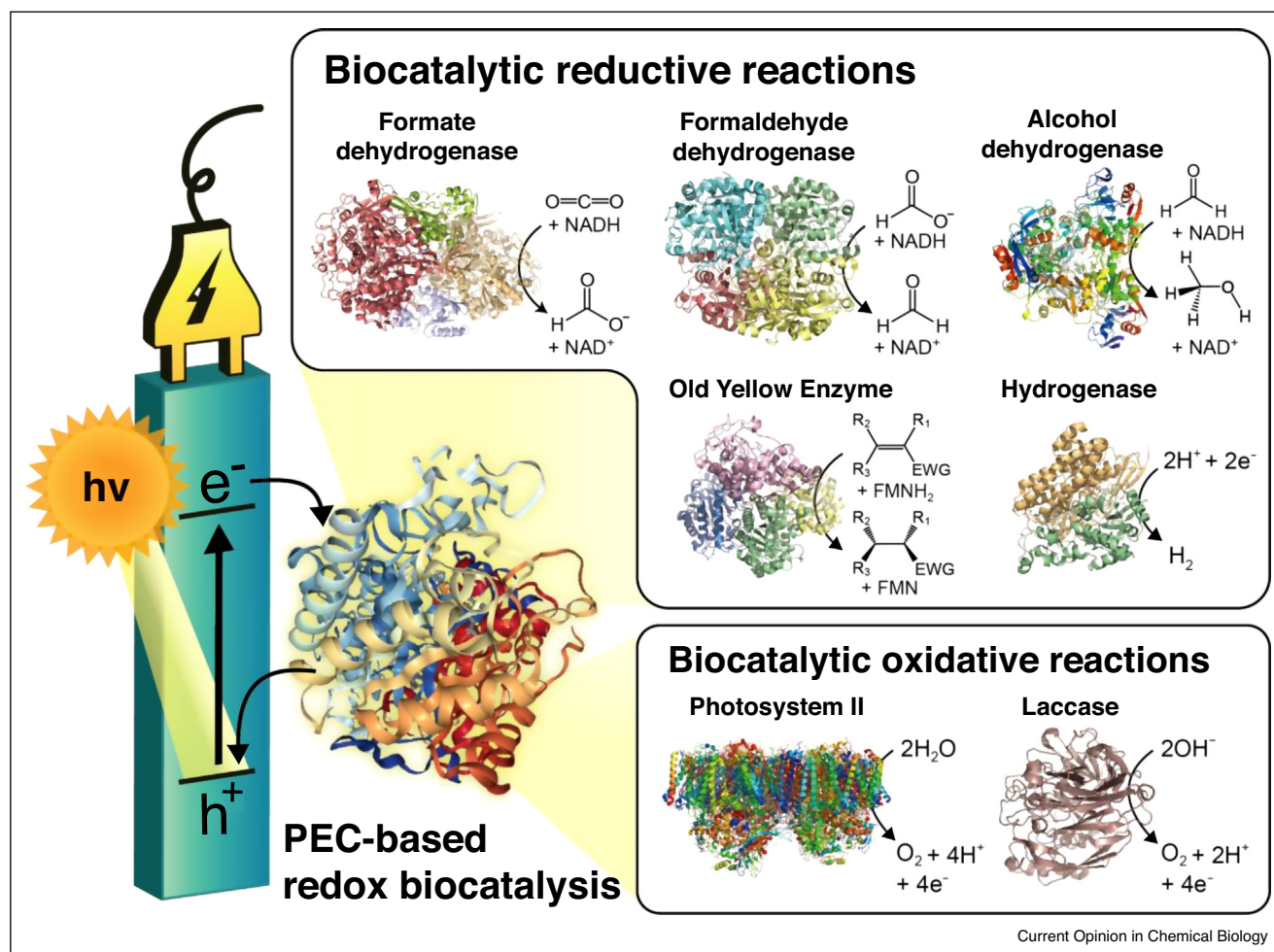
from) the enzyme prosthetic groups or adjoining electron relay centers via either an indirect or direct manner, as depicted in Figure 1. The biocatalytic PEC platforms based on indirect electron transfer are described in terms of the regeneration of NADH and FMNH<sub>2</sub>. Next, studies on direct transfer of charge carriers to (or from) oxidoreductases conjugated on (photo)electrodes are recounted in the order of the biocatalyzed oxidative and reductive reactions. Finally, we discuss future perspectives for advancing the PEC-based biotransformation approaches through the engineering of redox enzymes and photoelectrodes.

### Concept of biocatalytic photoelectrochemical platforms

The photoelectrode(s) in PEC platforms harness light energy and generate photoinduced electrons and holes with excited electronic potentials. A cathodic reaction of

interest (e.g. FMN reduction) can take place when the conduction band-edge potential of a photocathode is more negative than the redox potential of the reaction. In addition, the quasi-Fermi level for electrons must be more negative than the redox potential to increase the concentration of electrons that participate in the reductive reaction. The quasi-Fermi level is often not sufficient to drive the reductive reaction; thus, an external bias is applied to make the quasi-electrochemical potential more negative, accomplishing an otherwise-impossible reaction. The application of external voltage can modulate the quasi-Fermi level of the electrons to selectively drive a catalytic redox reaction of interest [20] and the degree of band bending to enhance separation and migration of photogenerated electron-hole pairs [21]. Band bending refers to the energetic variation of the bands at the semiconductor/electrolyte interface after the equalization of the Fermi level of the semiconductor's electrons and

Figure 1



Redox biotransformation driven by the cooperation of biocatalysis and photoelectrocatalysis. The photoexcited electrons can be delivered directly or indirectly to (or from) redox enzymes. The biocatalyzed reduction reactions performed by the biocatalytic PEC platforms include CO<sub>2</sub> reduction, *trans*-hydrogenation of C=C bonds, and H<sub>2</sub> evolution, whereas O<sub>2</sub> evolution is a major example of biocatalyzed oxidative reaction.

the redox potential of the electrolyte. Furthermore, physical separation of anodic and cathodic reaction sites provides advantages, such as the flexible combination of redox reactions (e.g. enzymatic reduction at a cathode and water oxidation at an anode), the proper tuning of reaction conditions (e.g. buffer types, pH, temperature, light on/off), the preservation of reduced redox cofactor (e.g. NADH, FMNH<sub>2</sub>) from oxidation at (photo)anodes, and the protection of enzymes from oxidative degradation at (photo)anodes.

The biocatalytic PEC platforms activate redox enzymes through photoinduced regeneration of diffusing cofactors or direct electron transfer to the enzymes that are conjugated to electrodes, as illustrated in Figure 2a. Three different configurations have been adopted: (i) photoanode/photocathode, (ii) anode/photocathode, and (iii) photoanode/cathode. These examples are listed in detail in Table 1. For example, in the photocathode/photoanode configuration, both photoelectrodes absorb light to generate photoexcited electron-hole pairs. At the photoanode, the photoexcited holes are consumed by water oxidation reaction, and the photoexcited electrons migrate through an external wire to the photocathode to fill the photoexcited holes. The remaining photoexcited electrons in the conduction band of the photocathode are transferred either to an electron mediator (for indirect electron transfer) or to the prosthetic group of an oxidoreductase (for direct electron transfer).

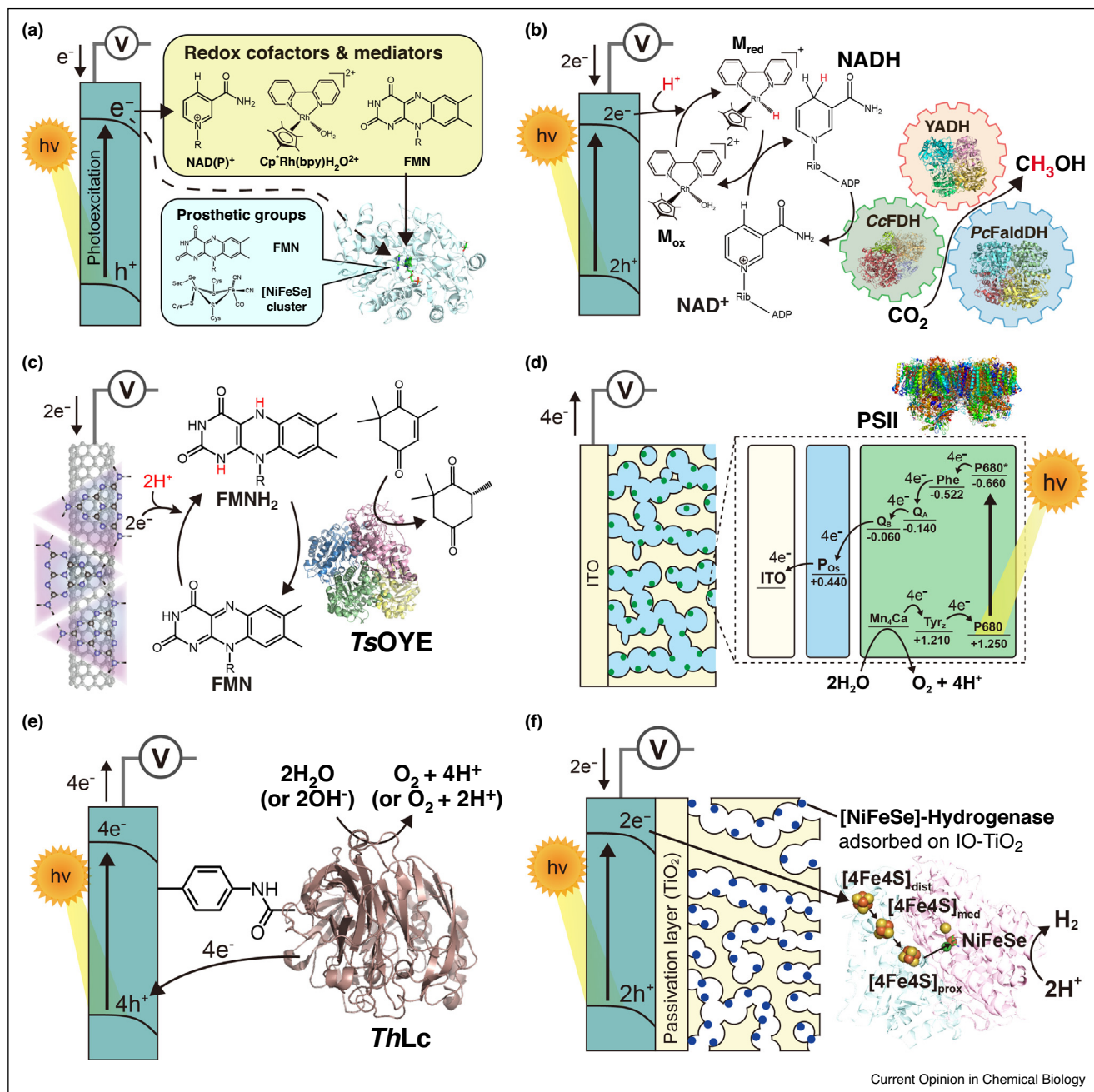
The most widely used photoelectrode material is a semiconductor (e.g. BiVO<sub>4</sub>, BiFeO<sub>3</sub>) that absorbs photons with energy higher than its bandgap energy and creates photoexcited charge carriers. The p-type semiconductors are more suitable for driving enzymatic reductive reactions than n-type semiconductors because photoexcited electrons in the conduction band are swept toward the semiconductor/electrolyte interface whereas holes move in the opposite direction. The introduction of a cocatalyst (e.g. Co–Pi, FeOOH, TiCo) on the light-harvesting semiconductor electrode can accelerate the catalytic reaction and decrease the overpotential associated with energy loss during charge migration and the low kinetics of a catalytic reaction by functioning as reaction sites and promoting charge separation [22]. In contrast, an electrode wired to natural photosynthetic complexes (such as photosystem [PS] I and II), thylakoid membranes, or cyanobacteria can also function as a photoelectrode, even though the electrode is not a semiconductor [23–27]. In the PS II-functionalized electrode, chromophores (e.g. chlorophylls and carotenoids within PS II) harness light energy, and then the photoexcited electrons are swept from the reaction center complex to an electrode over the course of O<sub>2</sub> evolution at the Mn<sub>4</sub>CaO<sub>5</sub> cluster [28\*,29].

### Photoelectrochemical regeneration of cofactors for redox biocatalysis

The sustainable delivery of photoexcited electrons to oxidoreductases via an indirect way is generally implemented through the regeneration of diffusing cofactors (or mediators) that relay electrons between photoelectrodes and oxidoreductases. The PEC regeneration of NAD(P)H has been applied to various oxidoreductases (e.g. ene-reductases, cytochrome P450 monooxygenases, formate dehydrogenases, Baeyer–Villiger monooxygenases) [2]. As direct electrocatalytic reduction of NAD<sup>+</sup> can form enzymatically inactive NAD<sub>2</sub> dimers and NADH isomers, suitable mediators are needed for the hydride transfer from a (photo)electrode to NAD<sup>+</sup>. The Rh-based mediator, Cp<sup>\*</sup>Rh(bpy)H<sub>2</sub>O<sup>2+</sup> (**M**), is the most popular mediator because it shows high regioselectivity for the generation of enzymatically active 1,4-NADH [4] and requires a milder reduction potential of –0.55 V (versus NHE, pH 7.0) than that of NAD<sup>+</sup> (≈–0.96 V versus NHE, pH 7.0) [6]. Note that the cathodic potential for NAD<sup>+</sup> reduction is much lower than the redox potential of NAD<sup>+</sup> (–0.32 V versus NHE, pH 7.0) because of the overpotential caused by the formation of NAD<sub>2</sub> dimers [30]. The Park group reported several different PEC platforms for photoanodic water oxidation to extract electrons and (photo)cathodic reduction of **M** to regenerate enzymatically active NADH [31\*\*,32\*\*,33–35]. For example, they designed a tandem PEC system coupled with a cascaded enzyme circuit made of three different dehydrogenases to produce methanol from CO<sub>2</sub> (Figure 2b). Dual illumination and applied voltage on photoelectrodes facilitated water oxidation and the regeneration of NADH via **M**, mimicking the Z-scheme of photoinduced electron transport in natural photosynthesis. The formation of methanol occurs through reversible hydrogenation reactions driven by the cooperation of the metal-containing dehydrogenases, and the efficient photoregeneration of NADH increased the NADH/NAD<sup>+</sup> ratio, shifting the domino reaction towards the methanol production. In addition, a superior formaldehyde dehydrogenase having a strong binding affinity to formate and a high formate assimilation activity was identified by screening using the Basic Local Alignment Search Tool and systematic sequence analysis, giving a much-enhanced production rate of methanol in the tandem PEC platform.

To circumvent the use of expensive NAD(P)H and hydride-transfer mediators (e.g. **M**), photoelectrochemical regeneration of FMNH<sub>2</sub> has been studied for the reduction of the prosthetic flavin groups in flavoenzymes (e.g. Old Yellow Enzyme, OYE) [36,37]. Note that the reduction potential of FMN (–0.24 V versus NHE, pH 7.0) is milder than those of NAD<sup>+</sup> and **M**, making the process energetically more feasible. Recently, Son *et al.* reported a biocatalytic PEC platform for the activation of an OYE from *Thermus scotoductus* (*TsOYE*) (Figure 2c)

Figure 2



Biocatalytic photoelectrochemical platforms for solar activation of oxidoreductases. **(a)** Photoactivation of redox enzymes through the regeneration of cofactor/mediator (marked by solid lines) and direct transfer of electrons to prosthetic groups (marked by a dashed line); **(b)** NADH regeneration for the three-dehydrogenase cascade to reduce  $CO_2$  to methanol [31\*\*]; **(c)**  $FMNH_2$  regeneration to deliver a hydride to  $TsOYE$  for highly enantioselective reduction of  $C=C$  bonds [38\*]; **(d)** Extraction of photoexcited electrons from PS II entrapped in an osmium complex-modified polymer for  $O_2$  evolution [41]. The numbers indicate voltages (versus NHE) at pH 6.5; **(e)** Extraction of electrons from  $ThLc$  conjugated to  $In_2S_3$  photoanode for  $O_2$  evolution [45\*]; **(f)** Transfer of photoexcited electrons to [NiFeSe]-hydrogenase adsorbed on  $p-Si|IO-TiO_2$  photocathode for  $H_2$  evolution [50\*\*].

[38\*]. Transition-metal-catalyzed asymmetric *trans*-hydrogenation was the subject of the 2001 Nobel prize in Chemistry, which can also be accomplished biocatalytically using  $TsOYE$  [39]. The PEC system extracted

electrons from solar-driven oxidation of water and delivered them to an electrocatalytic cathode for a two-electron reduction of  $FMN$  molecules. Subsequently,  $TsOYE$  was reduced by receiving the electrons from free

Table 1

A list of redox biotransformation by biocatalytic photoelectrochemical platforms. The descriptions of (photo)anodes and (photo)cathodes are arranged in the order of enzymes, electrode materials, and key redox reactions. Note that the light and dark reactions are highlighted by yellow background (with LIGHT mark at the upper right corner) and white background (with the DARK mark), respectively. Also listed are applied biases for each platform and the biotransformation performances, such as reaction rates, yields, turnover frequencies (TOFs), and total turnover numbers (TTNs).

(Photo)anode	(Photo)cathode	Applied voltage	Biocatalytic performance	Ref.
LIGHT <ul style="list-style-type: none"> <li>Electrode: Cobalt phosphate (Co-Pi)-deposited <math>\alpha</math>-Fe<sub>2</sub>O<sub>3</sub></li> <li>2H<sub>2</sub>O → O<sub>2</sub> + 4H<sup>+</sup> + 4e<sup>-</sup></li> </ul>	LIGHT <ul style="list-style-type: none"> <li>Enzymes: CcFDH (CO<sub>2</sub> + NADH → HCOO<sup>-</sup> + NAD<sup>+</sup>), PcFaldDH (HCOO<sup>-</sup> + NADH → HCHO + NAD<sup>+</sup>), YADH (HCHO + NADH → CH<sub>3</sub>OH + NAD<sup>+</sup>)</li> <li>Electrode: BiFeO<sub>3</sub></li> <li>(1) M<sup>2+</sup> + 2e<sup>-</sup> + H<sup>+</sup> → M<sup>+</sup></li> <li>(2) M<sup>+</sup> + NAD<sup>+</sup> → M<sup>2+</sup> + NADH</li> </ul>	0.6–1.0 V (two-electrode configuration)	<ul style="list-style-type: none"> <li>Initial reaction rate: ≈100 μM h<sup>-1</sup> (0.8 V, 2 h)</li> <li>Product concentration: ≈1310 μM (0.8 V, 6 h)</li> </ul>	[31**]
LIGHT <ul style="list-style-type: none"> <li>Electrode: Co-Pi-deposited, npp<sup>+</sup> triple junction silicon on indium tin oxide (ITO)</li> <li>2H<sub>2</sub>O → O<sub>2</sub> + 4H<sup>+</sup> + 4e<sup>-</sup></li> </ul>	LIGHT <ul style="list-style-type: none"> <li>Enzyme: TsFDH (CO<sub>2</sub> + NADH → HCOO<sup>-</sup> + NAD<sup>+</sup>)</li> <li>Electrode: hydrogen-terminated silicon nanowire</li> <li>(1) M<sup>2+</sup> + 2e<sup>-</sup> + H<sup>+</sup> → M<sup>+</sup></li> <li>(2) M<sup>+</sup> + NAD<sup>+</sup> → M<sup>2+</sup> + NADH</li> </ul>	1.5–1.8 V (two-electrode configuration)	<ul style="list-style-type: none"> <li>Initial reaction rate: ≈10 μM h<sup>-1</sup> (1.8 V, 1 h)</li> <li>Product concentration: 260 μM (1.8 V, 6 h)</li> </ul>	[33]
LIGHT <ul style="list-style-type: none"> <li>Electrode: FeOOH-deposited Fe<sub>2</sub>O<sub>3</sub> on fluorine-doped tin oxide (FTO)</li> <li>2H<sub>2</sub>O → O<sub>2</sub> + 4H<sup>+</sup> + 4e<sup>-</sup></li> </ul>	LIGHT <ul style="list-style-type: none"> <li>Enzyme: GDH (α-ketoglutarate + NADH + NH<sub>4</sub><sup>+</sup> → L-glutamate + NAD<sup>+</sup> + H<sub>2</sub>O)</li> <li>Electrode: Black silicon</li> <li>(1) M<sup>2+</sup> + 2e<sup>-</sup> + H<sup>+</sup> → M<sup>+</sup></li> <li>(2) M<sup>+</sup> + NAD<sup>+</sup> → M<sup>2+</sup> + NADH</li> </ul>	0.8–1.3 V (two-electrode configuration)	<ul style="list-style-type: none"> <li>Initial reaction rate: ≈200 μM h<sup>-1</sup> (1.2 V, 1 h)</li> <li>Yield: ≈16.2% (1.2 V, 5 h)</li> </ul>	[34]
LIGHT <ul style="list-style-type: none"> <li>Electrode: TiCo-deposited BiVO<sub>4</sub> on FTO</li> <li>2H<sub>2</sub>O → O<sub>2</sub> + 4H<sup>+</sup> + 4e<sup>-</sup></li> </ul>	LIGHT <ul style="list-style-type: none"> <li>Enzyme: [NiFeSe]-H<sub>2</sub>ase (2H<sup>+</sup> + 2e<sup>-</sup> → H<sub>2</sub>)</li> <li>Electrode: [NiFeSe]-H<sub>2</sub>ase on an inverse opal TiO<sub>2</sub>-coated p-type Si (p-Si O-TiO<sub>2</sub> H<sub>2</sub>ase)</li> <li>Direct electron transfer</li> </ul>	0.0–0.4 V (two-electrode configuration)	<ul style="list-style-type: none"> <li>Initial reaction rate: ≈0.28 μmol cm<sup>-2</sup> h<sup>-1</sup> (0.0 V, 1 h)</li> <li>H<sub>2</sub> production: ≈18.6 μmol cm<sup>-2</sup> (0.3 V, 5 h)</li> </ul>	[50**]
LIGHT <ul style="list-style-type: none"> <li>Electrode: Tandem assembly of FeOOH-deposited BiVO<sub>4</sub> and organometallic perovskite photovoltaic</li> <li>2H<sub>2</sub>O → O<sub>2</sub> + 4H<sup>+</sup> + 4e<sup>-</sup></li> </ul>	DARK <ul style="list-style-type: none"> <li>Enzyme: GDH (α-ketoglutarate + NADH + NH<sub>4</sub><sup>+</sup> → L-glutamate + NAD<sup>+</sup> + H<sub>2</sub>O)</li> <li>Electrode: Carbon nanotube film</li> <li>(1) M<sup>2+</sup> + 2e<sup>-</sup> + H<sup>+</sup> → M<sup>+</sup></li> <li>(2) M<sup>+</sup> + NAD<sup>+</sup> → M<sup>2+</sup> + NADH</li> </ul>	0.0 V (two-electrode configuration)	<ul style="list-style-type: none"> <li>Initial reaction rate: 2400 μM h<sup>-1</sup> (0.5 h)</li> <li>Yield: 81.5% (48 h)</li> <li>TOF<sub>GDH</sub>: 6200 h<sup>-1</sup> (0.5 h)</li> <li>TTN<sub>GDH</sub>: 108,800 (48 h)</li> </ul>	[32**]
LIGHT <ul style="list-style-type: none"> <li>Electrode: Co-Pi-deposited <math>\alpha</math>-Fe<sub>2</sub>O<sub>3</sub> on FTO</li> <li>2H<sub>2</sub>O → O<sub>2</sub> + 4H<sup>+</sup> + 4e<sup>-</sup></li> </ul>	DARK <ul style="list-style-type: none"> <li>Enzyme: TsFDH (CO<sub>2</sub> + NADH → HCOO<sup>-</sup> + NAD<sup>+</sup>)</li> <li>Electrode: ITO</li> <li>(1) M<sup>2+</sup> + 2e<sup>-</sup> + H<sup>+</sup> → M<sup>+</sup></li> <li>(2) M<sup>+</sup> + NAD<sup>+</sup> → M<sup>2+</sup> + NADH</li> </ul>	1.2–2.0 V (two-electrode configuration)	<ul style="list-style-type: none"> <li>Initial reaction rate: ≈8.2 μM h<sup>-1</sup> (1.2 V, 1 h)</li> <li>Product concentration: 550 μM (1.2 V, 5 h)</li> </ul>	[35]
LIGHT <ul style="list-style-type: none"> <li>Electrode: FeOOH-deposited BiVO<sub>4</sub> on ITO</li> <li>2H<sub>2</sub>O → O<sub>2</sub> + 4H<sup>+</sup> + 4e<sup>-</sup></li> </ul>	DARK <ul style="list-style-type: none"> <li>Enzyme: TsOYE [ketosiphonone + FMNH<sub>2</sub> → (R)-levodione + FMN]</li> <li>Electrode: protonated graphitic carbon nitride-hybridized carbon nanotube film</li> <li>FMN + 2e<sup>-</sup> + 2H<sup>+</sup> → FMNH<sub>2</sub></li> </ul>	0.3–0.9 V (two-electrode configuration)	<ul style="list-style-type: none"> <li>Average reaction rate: 1280 μM h<sup>-1</sup> (0.8 V, 2 h)</li> <li>Yield: 25.6% (0.8 V, 2 h)</li> <li>TOF<sub>TsOYE</sub>: ≈123 h<sup>-1</sup> (0.5 V, 0.5 h)</li> <li>TTN<sub>TsOYE</sub>: 256 (0.8 V, 2 h)</li> </ul>	[38*]
LIGHT <ul style="list-style-type: none"> <li>Photosynthetic unit: PS II (2H<sub>2</sub>O → O<sub>2</sub> + 4H<sup>+</sup> + 4e<sup>-</sup>)</li> <li>Electrode: PS II in Os complex-modified polymers on inverse opal ITO (IO-ITO P<sub>36</sub>-PSII)</li> <li>Direct electron transfer</li> </ul>	DARK <ul style="list-style-type: none"> <li>Electrode: platinum wire</li> <li>Cathodic reaction: not mentioned</li> </ul>	0.4–0.7 V vs. NHE (three-electrode configuration)	<ul style="list-style-type: none"> <li>Initial reaction rate: ≈0.12 μmol cm<sup>-2</sup> h<sup>-1</sup> (0.5 V, 0.5 h)</li> <li>O<sub>2</sub> evolution: 0.24 μmol cm<sup>-2</sup> (0.5 V, 1 h)</li> <li>TTN<sub>PSII</sub>: 946 (0.5 V, 1 h)</li> </ul>	[41]
LIGHT <ul style="list-style-type: none"> <li>Enzyme: ThLc (2H<sub>2</sub>O → O<sub>2</sub> + 4H<sup>+</sup> + 4e<sup>-</sup> or 2OH<sup>-</sup> → O<sub>2</sub> + 2H<sup>+</sup> + 4e<sup>-</sup>)</li> <li>Electrode: ThLc covalently attached to In<sub>2</sub>S<sub>3</sub>-coated FTO (FTO In<sub>2</sub>S<sub>3</sub> ThLc)</li> <li>Direct electron transfer</li> </ul>	DARK <ul style="list-style-type: none"> <li>Electrode: platinum wire</li> <li>Cathodic reaction: not mentioned</li> </ul>	0.8–1.0 V vs. NHE (three-electrode configuration)	<ul style="list-style-type: none"> <li>O<sub>2</sub> evolution: 0.93 nmol (1.0V, 0.1 h, unknown geometrical surface area)</li> </ul>	[45*]
DARK <ul style="list-style-type: none"> <li>Electrode: platinum wire</li> <li>Anodic reaction: not mentioned</li> </ul>	LIGHT <ul style="list-style-type: none"> <li>Enzyme: [NiFeSe]-H<sub>2</sub>ase (2H<sup>+</sup> + 2e<sup>-</sup> → H<sub>2</sub>)</li> <li>Electrode: [NiFeSe]-H<sub>2</sub>ase on a TiO<sub>2</sub>-coated p-type Si (p-Si TiO<sub>2</sub> H<sub>2</sub>ase)</li> <li>Direct electron transfer</li> </ul>	-0.1–0.5 V vs. NHE (three-electrode configuration)	<ul style="list-style-type: none"> <li>H<sub>2</sub> evolution: 0.025 μmol (-0.35V, 1 h, unknown geometrical surface area)</li> </ul>	[46]

≈, estimation; ~, range; CcFDH, formate dehydrogenase from *Clostridium carboxidivorans* P7T; PcFaldDH, formaldehyde dehydrogenase from *Pseudomonas cepacia* genomvar II; YADH, alcohol dehydrogenase from *Saccharomyces cerevisiae*; TsFDH, formate dehydrogenase from *Thiobacillus* sp. KNK65MA; GDH, L-glutamate dehydrogenase; H<sub>2</sub>ase, hydrogenase; ThLc, laccase from *Trametes hirsuta*.

FMNH<sub>2</sub>, successfully converting ketoisophorone to (*R*)-levodione (*ee*: 87.59%, production yield: 21.3%, TOF: 106 h<sup>-1</sup>, TTN: 213) under an applied bias of 0.5 V.

### Enzyme-conjugated electrodes for photoelectrochemical biotransformation

The conjugation of oxidoreductases to electrodes is an alternative method for injecting or withdrawing charge carriers at the interface of electrodes and redox enzymes. The characteristic redox properties of the prosthetic groups promote electrical communication between electrodes and oxidoreductases. Compared with the cofactor regeneration approaches, direct electron transfer is advantageous because (i) expensive cofactors or mediators are not needed, (ii) the electron pathway becomes simplified, minimizing energy loss and back electron transfer, and (iii) the redox potential of a prosthetic group is often less negative than those of cofactors to spend less energy on redox biocatalysis. Furthermore, the directionality of electron flow could be tuned by applying a bias to a photoelectrode. When the applied bias is more negative than the flatband potential ( $E_{FB}$ ) of the photoelectrode, the electron density increases, and the consequent band-bending is directed downward at the semiconductor/electrolyte interface [40<sup>\*</sup>]. This phenomenon facilitates the injection of the photoexcited electrons from the photoelectrode into the prosthetic group of oxidoreductases. When the applied bias is more positive than  $E_{FB}$ , the band-bending becomes upward, promoting the transfer of the electrons to the electrode.

Sokol *et al.* reported the positive-bias-driven activation of PS II entrapped in osmium complex-modified polymers on the surface of inverse opal indium tin oxide (IO-ITO|P<sub>O<sub>s</sub></sub>-PSII) under visible light (Figure 2d) [41]. PS II, a natural pigment–protein complex, is the benchmark photocatalyst for solar water oxidation [29]. Light harnessing by the pigments in PS II engenders charge formation and separation at the P680 primary electron donor site. The photogenerated holes are consumed at the oxygen-evolving complex to liberate O<sub>2</sub>, whereas the photogenerated electrons are transferred to the terminal electron acceptor plastoquinone B (Q<sub>B</sub>) [28<sup>\*</sup>]. The proper orientation of PS II on an electrode is vital for efficient transfer of electrons from Q<sub>B</sub> to the electrode under a positive applied voltage. To resolve the orientation issue, the researchers enfolded the PS II module by P<sub>O<sub>s</sub></sub> matrix, placing the redox Os<sup>2+/3+</sup> moieties in proximity to the photosynthetic units [42,43]. The homogeneously distributed Os centers mediated the transfer of photoexcited electrons from Q<sub>B</sub> to IO-ITO via an electron-hopping mechanism. Furthermore, the hierarchically structured inverse opal with exceptional high surface area allowed for more loading of PS II and P<sub>O<sub>s</sub></sub>, resulting in extensive interfacing between P<sub>O<sub>s</sub></sub> and ITO, and consequently effective wiring of PS II to the electrode.

The laccase from *Trametes hirsuta* (*ThLc*) is a copper-containing metalloenzyme that can electrocatalytically oxidize H<sub>2</sub>O (or OH<sup>-</sup>) to O<sub>2</sub>. The natural role of *ThLc* is to reduce O<sub>2</sub> to H<sub>2</sub>O, but a positive bias could reverse the direction in heterogeneous bioelectrocatalytic systems [44]. For example, Tapia *et al.* attached *ThLc* covalently to indium sulfide particles deposited on a fluorine-doped tin oxide electrode (FTO|In<sub>2</sub>S<sub>3</sub>|*ThLc*) for the evolution of O<sub>2</sub> (Figure 2e) [45<sup>\*</sup>]. The illumination on the *ThLc*-conjugated photoanode generated photoexcited holes on the valence band, which were annihilated by the electrons from the trinuclear copper cluster of *ThLc* under a positive voltage (0.8–1.0 V versus NHE). However, the vulnerability of *ThLc* to light and hydroxyl radicals terminated its biocatalytic activity after 6 min under the applied bias.

In contrast, a negative applied voltage can drive a reductive reaction via the injection of electrons to redox enzymes. For example, the Reisner group reported the photoactivation of [NiFeSe]-hydrogenase adsorbed on a titanium dioxide-coated p-type Si photocathode (p-Si|TiO<sub>2</sub>|H<sub>2</sub>ase) under a negative bias [46]. The [NiFeSe]-hydrogenase from *Desulfomicrobium baculatum* is a metalloenzyme that exhibits a strong kinetic tendency toward H<sub>2</sub> production in the presence of O<sub>2</sub> [47,48]. The photoexcited electrons generated from the p-Si|TiO<sub>2</sub> are delivered to the enzyme's [NiFeSe] active site via its intraprotein Fe–S cluster relays for the reduction of H<sup>+</sup> to H<sub>2</sub>. In the course of the photosynthetic reaction, the TiO<sub>2</sub> interlayer functioned as a biocompatible site for anchoring the hydrogenase, and the downward band-bending of p-type Si electrode expedited the transfer of photoexcited electrons toward the metal cluster of the enzyme [49]. In a recent follow-up study, the group replaced the planar TiO<sub>2</sub> by a hierarchical inverse opal TiO<sub>2</sub> layer to increase the amount of adsorbed [NiFeSe]-hydrogenases (Figure 2f) [50<sup>\*\*</sup>]. The biocatalytic photocathode was wired to a TiCo-deposited BiVO<sub>4</sub> photoanode to drive water splitting under a low bias. The high photovoltage of BiVO<sub>4</sub> accounted for a large portion of driving force to couple the biocatalyzed H<sub>2</sub> formation and the photoelectrochemical O<sub>2</sub> evolution.

### Conclusion and future perspectives

The biocatalytic PEC platform integrates biocatalysis and photoelectrocatalysis for sustainable redox biotransformations. The simultaneous employment of light and electrical energy tunes the directionality and the kinetics of photoexcited electrons for efficient activation of oxidoreductases. The PEC-based activation of redox enzymes occurs through either the regeneration of cofactors (e.g. NADH, FMNH<sub>2</sub>) or direct electron transfer on enzyme-conjugated electrodes. To be competitive with conventional enzymatic cofactor recycling methods, the biocatalytic PEC platforms should pursue swiftness, scalability, and sustainability. Critical issues relevant to the current

generation efficiency and the robustness of photoelectrodes and the proper interfacing of oxidoreductases to the PEC platforms should be addressed in future studies. The total turnover numbers of enzymatic NADH recycling are one or two orders of magnitude greater than those of PEC approaches [2]. The lower regeneration efficiency is ascribed to the fact that redox mediators are reduced at the surface of a photoelectrode, whereas homogeneously distributed secondary enzymes reduce NAD<sup>+</sup> over an entire reaction medium simultaneously. The limitation would be compensated by enhancing the kinetics of charge and mass transfer, increasing the surface-to-volume ratio of photoelectrodes, and designing more efficient redox mediators. The design of enzyme-hybrid photoelectrodes with a protective layer (e.g. photocorrosion-resistant oxide) having antifouling properties can be a promising strategy for minimizing undesirable back electron transfer and ensuring longer-term use of biocatalytic PEC platforms. As the active sites of oxidoreductases are often buried deep within polypeptides, it would be desirable for redox enzymes to possess a prosthetic group (or a redox relay center) near their surfaces to minimize the interfacial electron tunneling barrier. Such a structural modification may be implemented through the *de novo* computational enzyme design that can generate libraries of novel sequences and fashion a wide range of protein structures with atomic-level accuracy [51,52]. Finally, the development of heterostructured photoelectrodes by the combination of dissimilar semiconductors (e.g. perovskite solar cell) would boost the solar-to-chemical conversion efficiency and realize *bias-free* redox biocatalysis because the heterostructures offer effective charge separation and migration, enhancing current generation [53]. Furthermore, computer-aided design of robust enzymes having high specificity and stability should allow for scalable and durable biotransformation. Taken together, the multidisciplinary collaboration across enzyme engineering, photoelectrochemistry, and materials science should establish more efficient and sustainable PEC-based biotransformation processes.

### Conflict of interest statement

Nothing declared.

### Acknowledgement

This study was supported by the National Research Foundation (NRF) via the Creative Research Initiative Center (NRF-2015R1A3A2066191), Republic of Korea.

### References and recommended reading

Papers of particular interest, published within the period of review, have been highlighted as:

- of special interest
- of outstanding interest

1. Grogan G: **Synthesis of chiral amines using redox biocatalysis.** *Curr Opin Chem Biol* 2018, **43**:15-22.
2. Lee SH, Choi DS, Kuk SK, Park CB: **Photobiocatalysis: activating redox enzymes by direct or indirect transfer of photoinduced electrons.** *Angew Chem Int Ed* 2018, **57**:7958-7985.
3. Sheldon RA, Woodley JM: **Role of biocatalysis in sustainable chemistry.** *Chem Rev* 2018, **118**:801-838.
4. Hollmann F, Arends IWCE, Buehler K: **Biocatalytic redox reactions for organic synthesis: nonconventional regeneration methods.** *ChemCatChem* 2010, **2**:762-782.
5. Hollmann F, Arends IWCE, Holtmann D: **Enzymatic reductions for the chemist.** *Green Chem* 2011, **13**:2285-2314.
6. Wang X, Saba T, Yiu HHP, Howe RF, Anderson JA, Shi J: **Cofactor NAD(P)H regeneration inspired by heterogeneous pathways.** *Chem* 2017, **2**:621-654.
7. Hutton GAM, Reuillard B, Martindale BCM, Caputo CA, Lockwood CWJ, Butt JN, Reisner E: **Carbon dots as versatile photosensitizers for solar-driven catalysis with redox enzymes.** *J Am Chem Soc* 2016, **138**:16722-16730.
8. Brown KA, Wilker MB, Boehm M, Hamby H, Dukovic G, King PW: **Photocatalytic regeneration of nicotinamide cofactors by quantum dot-enzyme biohybrid complexes.** *ACS Catal* 2016, **6**:2201-2204.
9. Stufano P, Paris AR, Bocarsly A: **Photoelectrochemical NADH regeneration using Pt-modified p-GaAs semiconductor electrodes.** *ChemElectroChem* 2017, **4**:1066-1073.
10. Choi WS, Lee SH, Ko JW, Park CB: **Human urine-fueled light-driven NADH regeneration for redox biocatalysis.** *ChemSusChem* 2016, **9**:1559-1564.
11. Ji X, Wang J, Mei L, Tao W, Barrett A, Su Z, Wang S, Ma G, Shi J, Zhang S: **Porphyrin/SiO<sub>2</sub>/Cp\*Rh(bpy)Cl hybrid nanoparticles mimicking chloroplast with enhanced electronic energy transfer for biocatalyzed artificial photosynthesis.** *Adv Funct Mater* 2018, **28**:1705083.
12. Lee SH, Choi DS, Pesic M, Lee YW, Paul CE, Hollmann F, Park CB: **Cofactor-free, direct photoactivation of enoate reductases for the asymmetric reduction of C=C bonds.** *Angew Chem Int Ed* 2017, **56**:8681-8685.
13. Lee JH, Nam DH, Lee SH, Park JH, Park CB, Jeong KJ: **Solar-to-chemical conversion platform by robust cytochrome P450-P(3HB) complex.** *J Ind Eng Chem* 2016, **33**:28-32.
14. Wilker MB, Utterback JK, Greene S, Brown KA, Mulder DW, King PW, Dukovic G: **Role of surface-capping ligands in photoexcited electron transfer between CdS nanorods and [FeFe] hydrogenase and the subsequent H<sub>2</sub> generation.** *J Phys Chem C* 2018, **122**:741-750.
15. Ryu J, Lee SH, Nam DH, Park CB: **Rational design and engineering of quantum-dot-sensitized TiO<sub>2</sub> nanotube arrays for artificial photosynthesis.** *Adv Mater* 2011, **23**:1883-1888.
16. Lee SH, Ryu J, Nam DH, Park CB: **Photoenzymatic synthesis through sustainable NADH regeneration by SiO<sub>2</sub>-supported quantum dots.** *Chem Commun* 2011, **47**:4643-4645.
17. Nam DH, Lee SH, Park CB: **CdTe, CdSe, and CdS nanocrystals for highly efficient regeneration of nicotinamide cofactor under visible light.** *Small* 2010, **6**:922-926.
18. Kim J, Lee SH, Tieves F, Choi DS, Hollmann F, Paul C, Park CB: **Biocatalytic C=C bond reduction through carbon nanodot-sensitized regeneration of NADH analogues.** *Angew Chem Int Ed* 2018, **57**:13825-13828.
19. Ko JW, Choi WS, Kim J, Kuk SK, Lee SH, Park CB: **Self-assembled peptide-carbon nitride hydrogel as a light-responsive scaffold material.** *Biomacromolecules* 2017, **18**:3551-3556.
20. Li J, Wu N: **Semiconductor-based photocatalysts and photoelectrochemical cells for solar fuel generation: a review.** *Catal Sci Technol* 2015, **5**:1360-1384.
21. Jiang C, Moniz SJA, Wang A, Zhang T, Tang J: **Photoelectrochemical devices for solar water splitting – materials and challenges.** *Chem Soc Rev* 2017, **46**:4645-4660.

22. Yang J, Wang D, Han H, Li C: **Roles of cocatalysts in photocatalysis and photoelectrocatalysis**. *Acc Chem Res* 2013, **46**:1900-1909.
23. Ciornii D, Riedel M, Stieger KR, Feifel SC, Hejazi M, Lokstein H, Zouni A, Lisdat F: **Bioelectronic circuit on a 3D electrode architecture: enzymatic catalysis interconnected with photosystem I**. *J Am Chem Soc* 2017, **139**:16478-16481.
24. Efrati A, Lu C-H, Michaeli D, Nechushtai R, Alsaoub S, Schuhmann W, Willner I: **Assembly of photo-bioelectrochemical cells using photosystem I-functionalized electrodes**. *Nat Energy* 2016, **1**:15021.
25. Zhang JZ, Bombelli P, Sokol KP, Fantuzzi A, Rutherford AW, Howe CJ, Reisner E: **Photoelectrochemistry of photosystem II in vitro vs in vivo**. *J Am Chem Soc* 2018, **140**:6-9.
26. Pankratova G, Pankratov D, Di Bari C, Goñi-Urtiaga A, Toscano MD, Chi Q, Pita M, Gorton L, De Lacey AL: **Three-dimensional graphene matrix-supported and thylakoid membrane-based high-performance bioelectrochemical solar cell**. *ACS Appl Energy Mater* 2018, **1**:319-323.
27. Sekar N, Jain R, Yan Y, Ramasamy RP: **Enhanced photo-bioelectrochemical energy conversion by genetically engineered cyanobacteria**. *Biotechnol Bioeng* 2016, **113**:675-679.
28. Zhang JZ, Sokol KP, Paul N, Romero E, van Grondelle R, Reisner E: **Competing charge transfer pathways at the photosystem II-electrode interface**. *Nat Chem Biol* 2016, **12**:1046-1052.
- A study on the identification of photogenerated H<sub>2</sub>O<sub>2</sub> from O<sub>2</sub> by chlorophyll pigments and the concomitant charge leakages at the PSII-electrode interface, providing an insight into a rational design of pigment-containing photoelectrodes.
29. Kato M, Zhang JZ, Paul N, Reisner E: **Protein film photoelectrochemistry of the water oxidation enzyme photosystem II**. *Chem Soc Rev* 2014, **43**:6485-6497.
30. Gorton L, Domínguez E: **Electrochemistry of NAD(P)<sup>+</sup>/NAD(P)H**. In *Encyclopedia of Electrochemistry*. Edited by Wilson GS. Wiley-VCH; 2007:67-143.
31. Kuk SK, Singh RK, Nam DH, Singh R, Lee JK, Park CB: **Photoelectrochemical reduction of carbon dioxide to methanol through a highly efficient enzyme cascade**. *Angew Chem Int Ed* 2017, **56**:3827-3832.
- A benchmark contribution in photobiocatalytic reduction of CO<sub>2</sub> to methanol using three-dehydrogenase cascade.
32. Lee YW, Boonmongkolras P, Son EJ, Kim J, Lee SH, Kuk SK, Ko JW, Shin B, Park CB: **Unbiased biocatalytic solar-to-chemical conversion by FeOOH/BiVO<sub>4</sub>/perovskite tandem structure**. *Nat Commun* 2018, **9**:4208.
- Bias-free photoelectrochemical tandem configuration for redox biocatalysis using light as a sole energy source.
33. Son EJ, Ko JW, Kuk SK, Choe H, Lee S, Kim JH, Nam DH, Ryu GM, Kim YH, Park CB: **Sunlight-assisted, biocatalytic formate synthesis from CO<sub>2</sub> and water using silicon-based photoelectrochemical cells**. *Chem Commun* 2016, **52**:9723-9726.
34. Nam DH, Ryu GM, Kuk SK, Choi DS, Son EJ, Park CB: **Water oxidation-coupled, photoelectrochemical redox biocatalysis toward mimicking natural photosynthesis**. *Appl Catal B* 2016, **198**:311-317.
35. Nam DH, Kuk SK, Choe H, Lee S, Ko JW, Son EJ, Choi E-G, Kim YH, Park CB: **Enzymatic photosynthesis of formate from carbon dioxide coupled with highly efficient photoelectrochemical regeneration of nicotinamide cofactors**. *Green Chem* 2016, **18**:5989-5993.
36. Toogood HS, Knaus T, Scrutton NS: **Alternative hydride sources for ene-reductases: current trends**. *ChemCatChem* 2014, **6**:951-954.
37. Mifsud M, Gargiulo S, Iborra S, Arends IWCE, Hollmann F, Corma A: **Photobiocatalytic chemistry of oxidoreductases using water as the electron donor**. *Nature Commun* 2014, **5**:3145.
38. Son EJ, Lee SH, Kuk SK, Pesic M, Choi DS, Ko JW, Kim K, Hollmann F, Park CB: **Carbon nanotube-graphitic carbon nitride hybrid films for flavoenzyme-catalyzed photoelectrochemical cells**. *Adv Funct Mater* 2017, **28**:1705232.
- The first photoelectrochemical activation of TsOYE through the regeneration of free FMNH<sub>2</sub>.
39. Scholtissek A, Tischler D, Westphal AH, van Berkel WJH, Paul CE: **Old yellow enzyme-catalysed asymmetric hydrogenation: linking family roots with improved catalysis**. *Catalysts* 2017, **7**:130.
40. Bachmeier A, Wang VCC, Woolerton TW, Bell S, Fontecilla-Camps JC, Can M, Ragsdale SW, Chaudhary YS, Armstrong FA: **How light-harvesting semiconductors can alter the bias of reversible electrocatalysts in favor of H<sub>2</sub> production and CO<sub>2</sub> reduction**. *J Am Chem Soc* 2013, **135**:15026-15032.
- Tuning the directionality of the reversible biocatalysis driven by [NiFeSe]-hydrogenase and carbon monoxide dehydrogenase adsorbed on semiconductors.
41. Sokol KP, Mersch D, Hartmann V, Zhang JZ, Nowaczyk MM, Rogner M, Ruff A, Schuhmann W, Plumere N, Reisner E: **Rational wiring of photosystem II to hierarchical indium tin oxide electrodes using redox polymers**. *Energy Environ Sci* 2016, **9**:3698-3709.
42. Riedel M, Parak WJ, Ruff A, Schuhmann W, Lisdat F: **Light as trigger for biocatalysis: photonic wiring of flavin adenine dinucleotide-dependent glucose dehydrogenase to quantum dot-sensitized inverse opal TiO<sub>2</sub> architectures via redox polymers**. *ACS Catal* 2018, **8**:5212-5220.
43. Saboe PO, Conte E, Farell M, Bazan GC, Kumar M: **Biomimetic and bioinspired approaches for wiring enzymes to electrode interfaces**. *Energy Environ Sci* 2017, **10**:14-42.
44. Pita M, Mate DM, Gonzalez-Perez D, Shleev S, Fernandez VM, Alcalde M, De Lacey AL: **Bioelectrochemical oxidation of water**. *J Am Chem Soc* 2014, **136**:5892-5895.
45. Tapia C, Shleev S, Conesa JC, De Lacey AL, Pita M: **Laccase-catalyzed bioelectrochemical oxidation of water assisted with visible light**. *ACS Catal* 2017, **7**:4881-4889.
- Laccase application as an oxygen evolution biocatalyst in a photoelectrochemical platform.
46. Lee C-Y, Park HS, Fontecilla-Camps JC, Reisner E: **Photoelectrochemical H<sub>2</sub> evolution with a hydrogenase immobilized on a TiO<sub>2</sub>-protected silicon electrode**. *Angew Chem Int Ed* 2016, **55**:5971-5974.
47. Wombwell C, Caputo CA, Reisner E: **[NiFeSe]-hydrogenase chemistry**. *Acc Chem Res* 2015, **48**:2858-2865.
48. Mersch D, Lee C-Y, Zhang JZ, Brinkert K, Fontecilla-Camps JC, Rutherford AW, Reisner E: **Wiring of photosystem II to hydrogenase for photoelectrochemical water splitting**. *J Am Chem Soc* 2015, **137**:8541-8549.
49. Lee SH, Ryu GM, Nam DH, Kim JH, Park CB: **Silicon nanowire photocathodes for light-driven electroenzymatic synthesis**. *ChemSusChem* 2014, **7**:3007-3011.
50. Nam DH, Zhang J, Andrei V, Kornienko N, Heidary N, Wagner A, Nakanishi K, Sokol K, Slater B, Zebger I et al.: **Solar water splitting with a hydrogenase integrated in photoelectrochemical tandem cells**. *Angew Chem Int Ed* 2018, **57**:10595-10599.
- Coupling the hydrogenase-catalyzed generation of H<sub>2</sub> with the BiVO<sub>4</sub>-catalyzed evolution of O<sub>2</sub> under visible light and low bias.
51. Huang P-S, Boyken SE, Baker D: **The coming of age of de novo protein design**. *Nature* 2016, **537**:320.
52. Zanghellini A: **De novo computational enzyme design**. *Curr Opin Biotechnol* 2014, **29**:132-138.
53. Sivula K, van de Krol R: **Semiconducting materials for photoelectrochemical energy conversion**. *Nat Rev Mater* 2016, **1**:15010.